Journal of Civil Engineering and Urban Planning (2023)
Clausius Scientific Press, Canada

DOI: 10.23977/jceup.2023.051002
ISSN 2616-3969 Vol. 5 Num. 10

Inferred Geological Data and Stability Analysis of Tunnel Surrounding Rock by Drilling and Blasting Method Based on Digital Twin

Liu Jian[1], Zhou Tong[1,*], Huang Xianbin[2], Zhang Keqin[3], Zhang Min[4]

[1]China Power Construction Jijiao Expressway Investment and Development Co., Ltd., Shijiazhuang, 050051, China
[2]Shanghai Municipal Engineering Design and Research Institute (Group) Co. Ltd., Shanghai, 200092, China
[3]School of Architecture and Civil Engineering, Xi'an University of Science and Technology, Xi'an, 710054, China
[4]Shudao Investment Group Co., Ltd., Chengdu, 610000, China
[*]Corresponding author

Keywords: Digital twin; Tunnel surrounding rock; Bayesian theory; Rock classification; Geological information inference

Abstract: Digital twin technology is commonly applied in tunnel engineering to manage and design mechanical and electrical equipment. However, the geological data of the tunnel surrounding rock during construction can also be inferred using digital twin models, providing a reference for tunnel construction and stability analysis. First, the structural information of the tunnel face is obtained through 3D laser scanning and point cloud analysis, establishing a digital twin model of the tunnel face. Then, an intelligent classification model of the rock mass is established by combining the collected prior information of the rock mass with Bayesian networks and junction tree algorithms. Formulas are developed to correlate the rock mass deformation modulus with the classification standard GSI, RMR, and BQ. The deformation modulus of the rock mass is inferred based on the measured field information and empirical data using Bayesian inference combined with Markov Chain Monte Carlo simulation, achieving a posterior probability distribution. Finally, this method is applied to the Dongpo Tunnel of the Taihang Expressway, with an accuracy rate of over 85% for rock mass classification. The inferred parameters of the rock mass deformation modulus are obtained using the prior information provided by the rock mass classification. Finite element modelling is conducted based on the inferred geological information, preliminarily establishing that the stability of the surrounding rock mass in the Dongpo Tunnel is relatively good.

1. Introduction

With the development of tunnel engineering, the construction of high-difficulty and high-risk tunnel projects in complex geological and hydrogeological environments is increasing [1]. As the main

environmental medium of tunnel engineering, the rock mass plays a crucial role in tunnel stability, and it is necessary to understand the properties of the surrounding rock mass throughout the entire lifespan of the tunnel to rationally select construction methods, support design parameters, and maintenance plans [2].

The digital twin is a technology that models, simulates, and analyses physical objects in the real world through digital means. By using sensors, wireless communication, and cloud computing, real-time data from real objects are collected and processed and compared and analysed with digital models [3]. With the gradual development of digitization in geotechnical engineering [4-5], the introduction of digital twin technology in tunnel engineering has been correspondingly researched. Lee [6] used BIM and GIS methods to establish a digital twin model of a tunnel for the detection, monitoring, and diagnosis of tunnel risks and abnormalities. Yu [7] used digital twin technology to monitor mechanical equipment failures in tunnels and successfully applied it to the Wenyi Road Tunnel in Hangzhou. Shen [8] used digital twin methods to establish a lighting environment model for tunnels to improve interior lighting design, which was applied to newly built tunnels in Hangzhou, reducing the accident rate to 3%. Currently, the application of digital twins mainly focuses on the design and management of tunnel machinery and equipment. In fact, after collecting the rock mass information required for digital twin modelling, the tunnel rock mass data can be evaluated and inferred based on the collected information, and a numerical analysis model of the tunnel can be established to calculate the mechanical characteristics of the tunnel and lining and analyse the stability of the tunnel rock mass [9].

Based on the tunnel digital twin model, there is an issue of insufficient rock mass information for rock classification. To address this, Zhou [10] constructed a rock mass quality evaluation and analysis model based on the Q-system classification method, combined with field measurement data and Bayesian networks. Xiao [11] established a method for determining the probability interval of the Geological Strength Index (GSI) using interval theory and Bayesian networks based on the quantitative relationship between rock block volume (Vb), joint surface coefficient (Jc), and GSI.

The process of inferring rock mass parameters based on the tunnel digital twin model is stochastic, and commonly used empirical methods also have model uncertainties. Therefore, Cai [12] used Monte Carlo sampling to obtain the strength and deformation statistical parameters of a rock mass based on uncertainty and applied them to the probabilistic design of rock engineering. Sari [13] considered the uncertainty of inferred rock mass property parameters using a probabilistic approach and predicted the strength of the rock mass using a probabilistic spreadsheet model. Feng [14] used the Bayesian method to predict the elastic modulus of rocks based on their uniaxial compressive strength. Wang [15-16] adopted the Bayesian method to select and describe the uncertainty relationship between the uniaxial compressive strength and elastic modulus through regression models.

Based on a summary of existing research, this study applies the digital twin model to infer the geological information of tunnel surrounding rock mass. Simultaneously, a Bayesian network is utilized to propose an empirical formula and data fusion algorithm for inferring rock mass parameters. The obtained geological information is then used to establish a numerical model to analyse tunnel deformation and stability.

2. Tunnel face information acquisition

Three-dimensional (3D) laser scanning technology instantaneously measures the spatial 3D coordinate values of a target object through the principle of laser ranging. By using the acquired spatial point cloud data, it can quickly establish a 3D visualization model of complex and irregular scenes. It has the advantages of high authenticity, high data sampling rate, high resolution, high accuracy, no time and space constraints, and easy postprocessing and output.

In this study, a Leica ScanStation P30 laser scanner was used to scan the tunnel face. The laser scanner was set up approximately 10 meters in front of the tunnel face, adjusted to a horizontal position, and fixed. The scanning accuracy and angle were set, and the tunnel face was scanned at a high density. When the scanning accuracy was set to 1.6 mm@10 m, it took approximately 2 minutes to complete the scanning of the entire tunnel face.

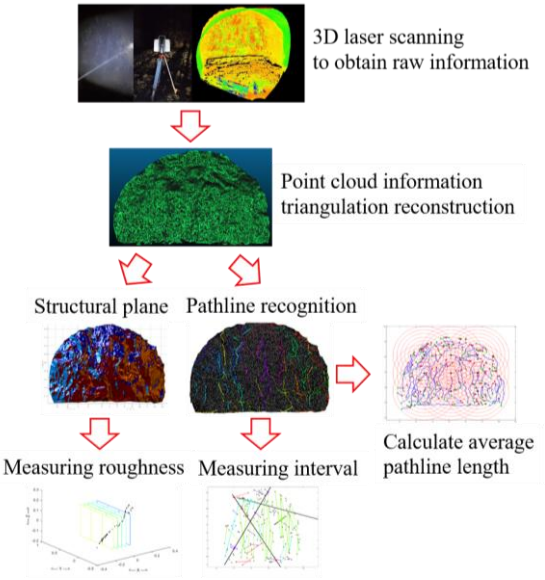

Figure 1: Information extraction process of tunnel face

After obtaining the point cloud information of the tunnel face using the 3D laser scanner, the automated rock mass information extraction method proposed in references [5] and [17-19] was applied. The point cloud format was converted (to PLY format) using CloudCompare, and Halcon was used for point cloud data preprocessing, resampling, denoising, and triangulation. Finally, the MATLAB program for automated rock mass information extraction was used to obtain the grouping information, spacing, joint inclination, pathline length, and roughness of the rock mass structural planes according to the process shown in Fig. 1.

3. Geological information inference for the surrounding rock

3.1 Intelligent classification of rock mass

Table 1: Comparison of GSI, BQ, and RMR14 classification standards

	Ave Distance	Num Group	Trace Length	Surface Condition	UCS	Water	Slake Durability
GSI	√	√		√			
BQ	√	√			√	√	
RMR14	√	√	√	√	√	√	√

Different rock mass classification methods consider different factors. The GSI method [20-21], BQ method [22], and RMR14 method [23-24] were selected for comparison, as shown in Tab. 1. It is difficult to evaluate multiparameter rock mass classification methods when there is insufficient rock mass information on site.

Eleven basic parameters, including volume joint number Jv (joint average distance: AveDistance, joint group number: NumGroup), joint path length: TraceLength, structural plane condition: SurfaceCondition (roughness of structural plane: Roughness, weathering degree of structural plane:

Weathering, infilling properties of structural plane: Infilling), unconfined compressive strength: UCS, slake durability index: SlakeDurability, and groundwater distribution characteristics: Water, as well as the rock mass quality evaluation indicators GSI, BQ, and RMR14, were selected. Based on the rock mass quality information of 260 groups [25], the collected tunnel surrounding rock classification case data were input into the network model using Netica software. The rock mass classification evaluation model was obtained by using the expectation maximization algorithm to learn the parameter values of the nodes (Fig. 2). This process solidifies the empirical experience of rock mass classification and provides support for tunnel engineering rock mass classification.

Based on this rock mass classification evaluation model, the conditional probability values of each node under given conditions can be obtained using the junction tree algorithm [26-27]. The specific steps are as follows: (1) establish a junction tree based on the existing Bayesian network; (2) use message propagation algorithms to transmit information along the junction tree; and (3) respond to results based on the given conditions.

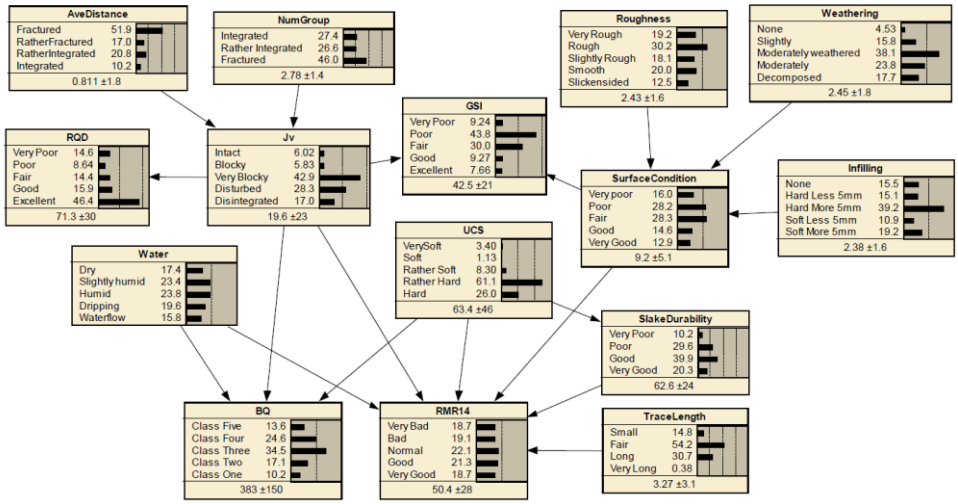

Figure 2: Rock mass classification evaluation model

3.2 Parameter inference of rock mass

Determining the deformation modulus of a rock mass on-site is time-consuming and laborious. When conducting reliable design for the underground structure of a rock mass, the probability distribution information of parameters is often needed. However, it is difficult to obtain meaningful statistical parameters from on-site test data. Therefore, in this section, Bayesian inference methods are introduced to consider empirical (prior) information from similar sites and use empirical formulas and on-site measured parameters to obtain the (posterior) probability distribution of the rock mass deformation modulus, guiding the selection of statistical parameters of the rock mass deformation modulus at engineering sites.

3.2.1 Formulas for rock mass deformation modulus - Classification standard

Combining commonly used rock mass quality evaluation methods, empirical formulas between the rock mass deformation modulus (Erm) and rock mass classification standards GSI, RMR, and BQ are established. To obtain universally applicable empirical formulas, engineering data are statistically analysed. Three commonly used models (linear, power-law, exponential) are used to describe the relationships between Erm-GSI, Erm-RMR, and Erm-BQ. The model parameters are optimized through the maximum likelihood method (Equation 1). Then, by comparing the values of the Akaike

Information Criterion (AIC) and Bayesian Information Criterion (BIC) [28], the performance of the models is evaluated to obtain the best formulas. The corresponding results are shown in Tab. 2.

$$L(\Theta) = \prod_{i=1}^{n} \frac{1}{E_{rm,i}\sqrt{2\pi}\sigma_t} \exp\left[-\frac{(\ln(E_{rm,i}) - \ln(\mu_i))^2}{2\sigma_t^2} \right] \quad (1)$$

where L(Θ) represents the likelihood function of the model corresponding to observed values (samples) of Erm. Erm,i represents the i-th observed value, μi represents the predicted mean of Erm based on the given classification standards (GSI, RMR, and BQ), and σt reflects the model error.

Table 2: Erm-RMR,Erm-GSI,Erm-BQ experience formulas

	Model	Formula	σt	Maximum likelihood value	AIC	BIC	Rank
Erm-GSI	Linear	Erm = 0.1245GSI	1.1973	1319.7	2641.4	2645.32	3
	Power-law	Erm = 2.1384×10-5GSI 3.1448	0.9424	1230.8	2465.6	2473.43	2
	Exponential	Erm = 0.1263e0.0673GSI	0.9338	1227.5	2459	2466.83	1
Erm-RMR	Linear	Erm = 0.1445RMR	0.9456	1482	2966	2970.04	3
	Power-law	Erm = 3.4477×10-5RMR 3.0337	0.753	1386.7	2777.4	2785.48	2
	Exponential	Erm = 0.2069 e0.0599RMR	0.7297	1373.6	2751.2	2759.28	1
Erm-BQ	Linear	Erm = 0.02665(BQ-90)	0.8240	1651.21	3304.42	3308.64	3
	Power-law	Erm = 3.53×10-4(BQ-90) 1.759	0.6883	1604.55	3213.10	3221.53	2
	Exponential	Erm = 0.7776 e0.00702(BQ-90)	0.8146	1586.91	3177.82	3186.25	1

3.2.2 Bayesian inference of rock mass deformation modulus

The rock mass deformation modulus, $E_{rm} = \exp(\mu_N + \sigma_N z)$, is defined as a lognormal distribution with a mean of $\mu = e^{\mu_N + \sigma_N^2/2}$ and a standard deviation of $\sigma = \sqrt{(e^{\sigma_N^2} - 1)e^{2\mu_N + \sigma_N^2}}$. The parameters μ and σ are estimated using prior information (engineering experience) and field measurements (GSI, RMR, and BQ). The joint conditional probability distribution function, P(μ, σ|Data,Prior), represents the probability of the parameters μ and σ given the prior and field measurement information. By applying the Bayesian theorem [29], the probability distribution function, PDF, of the rock mass deformation modulus, Erm, can be expressed as follows:

$$P(E_{rm} \mid \text{Data}, \text{Prior}) = K \int_{\mu,\sigma} P(E_{rm} \mid \mu, \sigma) P(\text{Data} \mid \mu, \sigma) P(\mu, \sigma) d\mu d\sigma \quad (2)$$

where K=(∫μ,σP(Data|μ,σ)P(μ,σ)dμdσ)-1 is the normalization constant ensuring that the integral of P(μ,σ|Data) equals 1. Data represent a set of field-tested rock mass data, P(Data|μ,σ) is the likelihood function reflecting the model's fit to the data, and P(μ,σ) is the prior probability distribution of μ and σ.

The posterior probability distribution of Erm, P(Erm|Data, Prior), is complex and difficult to obtain analytically. This study utilized the Markov Chain Monte Carlo (MCMC) simulation method along with the Metropolis–Hastings (MH) sampling technique [30-31]. A large number of random samples are generated according to Equation 2, and when the MCMC algorithm satisfies the detailed balance condition, statistical analysis of the generated samples yields the posterior probability distribution

P(Erm|Data, Prior).

For a specific engineering site, different empirical formulas and field measurements in Tab. 2 will yield different predicted values of the rock mass deformation modulus. The Bayesian inference method is used to integrate and update the predictions from different empirical formulas according to the following equation:

$$\frac{1}{\sigma^2} = \frac{1}{\sigma_i^2} + \frac{1}{\sigma_j^2} \tag{3}$$

$$\mu = \frac{\frac{1}{\sigma_i^2}\mu_i + \frac{1}{\sigma_j^2}\mu_j}{\frac{1}{\sigma_i^2} + \frac{1}{\sigma_j^2}} \tag{4}$$

where μi, μj, σi, and σj represent the mean and standard deviation of the i-th and j-th model predictions, and μ and σ represent the updated mean and standard deviation after Bayesian updating.

4. Engineering case study

This study constructs a digital twin model of a drill and blast tunnel to infer its geological information, classify the rock mass, establish a numerical model, and analyse the tunnel stability using the finite element method. The main workflow is shown in Fig. 3. To validate the applicability of this method, it is applied to verify the approach using the Dongpo Tunnel section of the Taihang Mountain Expressway in Handan.

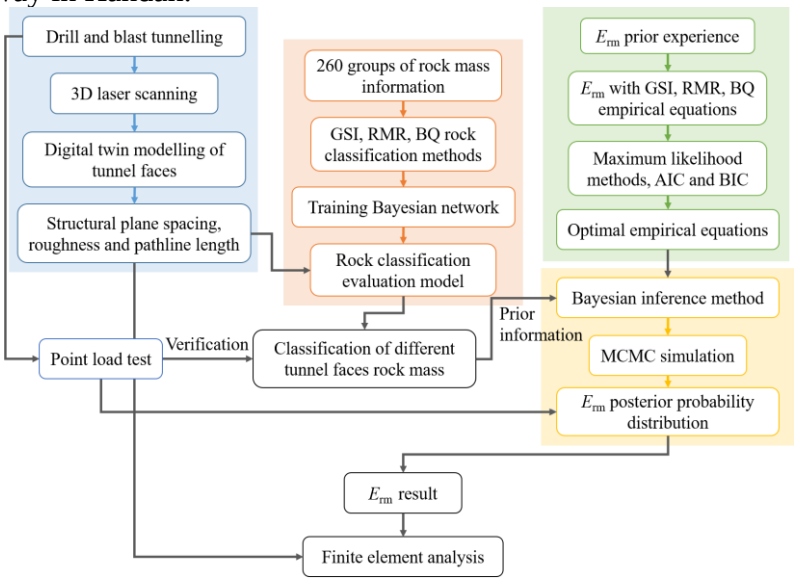

Figure 3: Work flow chart

The Dongpo Tunnel is a separating long tunnel (left tunnel: 3116 m, right tunnel: 3128 m) located in Lingdi Village and Dongpo Village, Yetao Town, Wu'an, Handan City, Hebei Province, as shown in Fig. 4. The geology in the tunnel area mainly consists of Quaternary overburden and Middle Ordovician Majiagou Formation thick-bedded to very thick-bedded dolomite and middle Cambrian Fengshan Formation thick-bedded limestone interbedded with thick-bedded sandstone and thin-bedded mudstone. The surrounding rock during tunnel excavation mainly comprises the Middle Cambrian Fengshan Formation thick-bedded limestone interbedded with thick-bedded sandstone and thin-bedded mudstone, with varying degrees of weathering from strong weathering to moderate weathering.

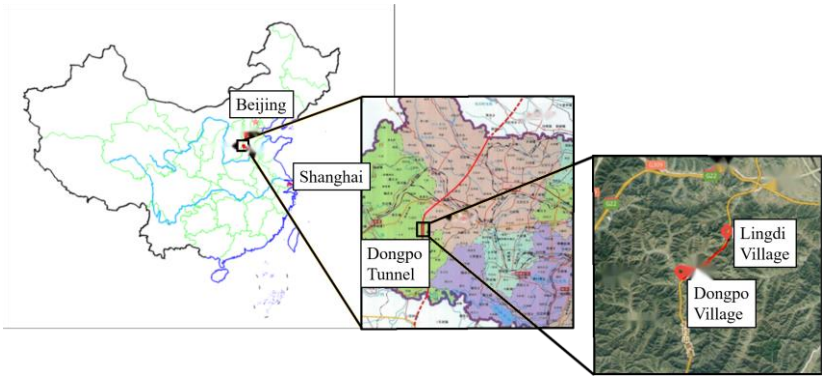

Figure 4: Geographical location of Dongpo Tunnel

4.1 Digital Twin Model

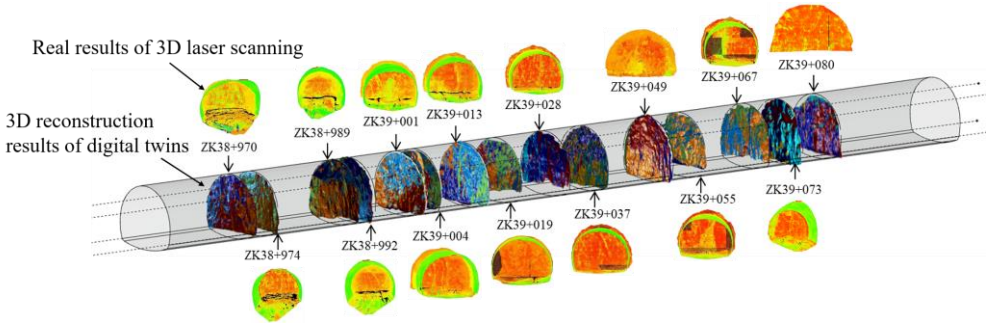

Figure 5: Digital twin model of the Dongpo tunnel face

Based on the method described in section 2, the main tunnel face of the drill and blast excavation in the Dongpo Tunnel is digitally twinned. First, the true structure of the tunnel face is obtained through 3D laser scanning, and then a digital twin reconstructs the structural plane of the tunnel face using 3D point cloud data (Fig. 5). This provides the raw data for rock mass classification and information inference.

4.2 Rock mass classification evaluation

Based on the information on rock strength obtained from the on-site point load test in the tunnel, the rock mass quality of 15 tunnel faces from ZK38+970 to ZK39+080 on the left side of the Dongpo Tunnel is evaluated. The BQ index Kv value is obtained through linear interpolation, and RMR14 is calculated using the method in reference [32]. At the same time, the rock mass is intelligently classified based on the established digital twin model using the method in section 3.1. The comparison results between the two are shown in Fig. 6. The rock mass classification evaluation results obtained using the classification model in section 3.1 are consistent with the on-site tested rock mass classification results. The accuracy rate of the BQ evaluation index reaches 100%, and the results obtained from the GSI and RMR14 evaluation indexes differ by only one level. The evaluation scores for the sections where the rating deviates are close to the peripheral rock mass. The prediction accuracy of the probability model is 93% and 87%, both above 85%, which verifies the applicability and accuracy of the rock mass classification evaluation method proposed in this study for evaluating this section of rock mass.

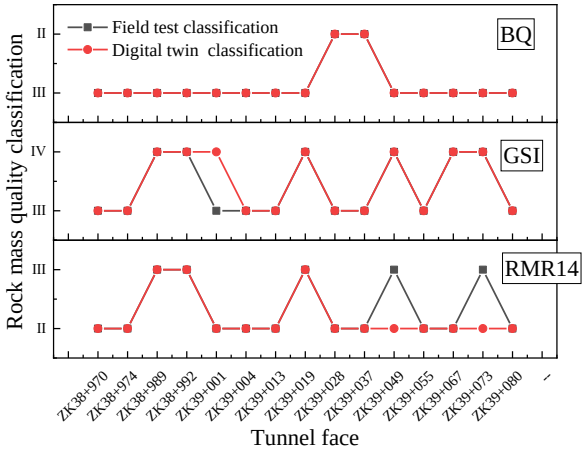

Figure 6: Rock mass quality classification of the Dongpo tunnel face

4.3 Finite element analysis

4.3.1 Model parameters

For the left side of the Dongpo Tunnel, full-section blasting excavation is adopted. After rock blasting excavation and slag removal, the initial lining (rigid arch, shotcrete) is constructed. After the deformation of the initial lining stabilizes, the construction of the inverted arch and secondary lining is carried out. To simulate the construction process, a finite element model with a length of 80 m, height of 70 m, and longitudinal extension of 110 m is established (Fig. 7). Considering the actual conditions of on-site construction, the excavation of the inverted arch and the construction of the secondary lining are relatively delayed (according to the on-site construction conditions, the delay is over 100 m). Therefore, the excavation of the inverted arch and the effect of the secondary lining are not considered during the simulation. According to the survey report, the surrounding rock of this construction section is limestone, with a rock mass parameter mi of 7, a Poisson's ratio of 0.25, and a density of 2750 kg/m3 [33-34]. The prior empirical rock mass deformation modulus is obtained based on reference [22], and the physical and mechanical parameters of the excavation part and the peripheral rock mass are determined by on-site laser scanning and point load test results using the method in section 3.2, as shown in Tabs. 3 and 4. The MATLAB program used for inferring rock mass parameters is shown in Fig. 8. The design parameters for the lining support and backfilling materials of the Dongpo Tunnel are listed in Tab. 5.

The generalized three-dimensional nonlinear Hoek–Brown strength criterion (Equation 5) is used to simulate the rock mass, and the plastic flow rule based on the improved Euler midpoint integration algorithm and the segmented implicit corrected plastic potential function is applied [35-36].

$$\frac{1}{\sigma_c^{(1/a-1)}}\left(\frac{3}{\sqrt{2}}\tau_{oct}\right)^{1/a}+\frac{m_b}{2}\left(\frac{3}{\sqrt{2}}\tau_{\mathrm{oct}}\right)-m_b\sigma_{\mathrm{m},2}=s\sigma_{\mathrm{c}} \tag{5}$$

where mb, s, and a are empirical parameters reflecting rock mass characteristics, mb is a dimensionless empirical parameter for different rock masses[35], σc is the uniaxial compressive strength of the rock, and σm,2 is the arithmetic mean of the first and third principal stresses. Parameter s reflects the degree of rock fragmentation[36]. As shown in Tab 3, Tab 4 and Tab 5.

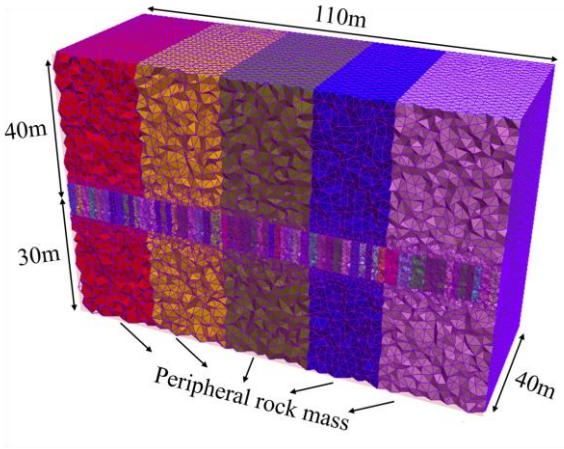

Figure 7: Mesh division of the finite element model

Table 3: Parameters of the excavated rock mass of the Dongpo tunnel

Serial number	Initial mileage	Termination mileage	UCS(MPa)	GSI	Erm(GPa)
1	ZK38+970	ZK38+974	30.09	52.7	5.95
2	ZK38+974	ZK38+989	47.29	54.04	8.22
3	ZK38+989	ZK38+992	28.61	34.87	4.18
4	ZK38+992	ZK39+001	32.40	29.59	3.81
5	ZK39+001	ZK39+004	39.72	43.9	5.85
6	ZK39+004	ZK39+013	46.24	45.64	6.10
7	ZK39+013	ZK39+019	37.38	51.77	6.52
8	ZK39+019	ZK39+028	37.38	37.19	4.64
9	ZK39+028	ZK39+037	70.21	50.73	10.49
10	ZK39+037	ZK39+049	63.71	43.95	7.85
11	ZK39+049	ZK39+055	42.78	37.53	4.86
12	ZK39+055	ZK39+067	45.19	46.33	6.47
13	ZK39+067	ZK39+073	42.66	36.98	4.92
14	ZK39+073	ZK39+080	37.50	34.77	4.35

Table 4: Parameters of the peripheral rock mass of the Dongpo tunnel

Serial number	Initial mileage	Termination mileage	UCS(MPa)	GSI	Erm(GPa)
1	ZK38+970	ZK38+992	35.33	47.20	6.12
2	ZK38+992	ZK39+013	39.45	39.71	5.25
3	ZK39+013	ZK39+037	48.33	46.56	7.22
4	ZK39+037	ZK39+055	53.24	40.74	6.36
5	ZK39+055	ZK39+080	41.74	43.80	5.55

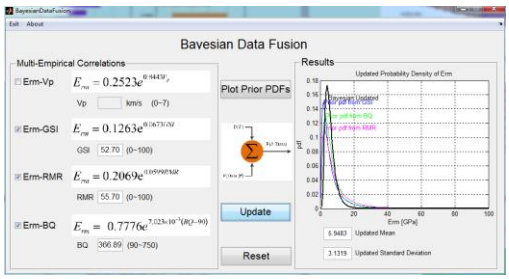

(a) Excavated rock mass (ZK38+970 ~ ZK38+974)

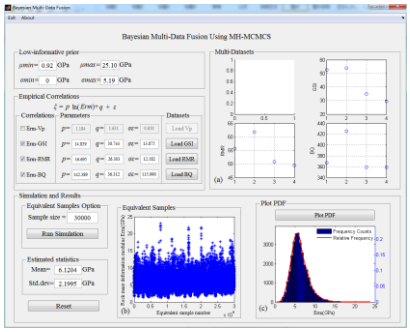

(b) Peripheral rock mass (ZK38+970 ~ ZK38+992)

Figure 8: Geological parameter inference program of tunnel surrounding rock

Table 5: Lining and backfill material parameters of Dongpo tunnel

	Density (kg/m3)	Elasticity modulus (GPa)	Poisson's ratio	Thicknesses (cm)
Primary lining	2500	28.0	0.20	25
Secondary lining	2500	29.5	0.25	40
Backfill	2600	26.0	0.25	-

4.3.2 Results and analysis

According to the results of the finite element analysis, the deformation of the tunnel is shown in Fig. 9. The dynamic variation curves of the relative displacement of the tunnel sidewalls, displacement of the tunnel roof, and deformation of the tunnel face during the construction process are shown in Fig. 10. The internal force distribution of the lining is shown in Fig. 11.

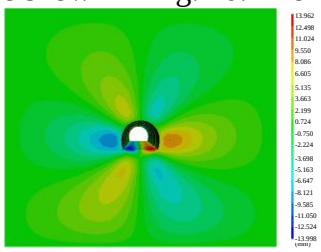

(a) Horizontal deformation

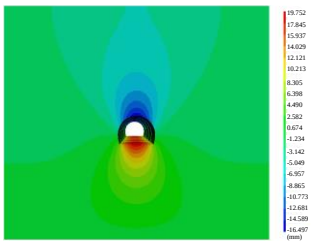

(b) Vertical deformation

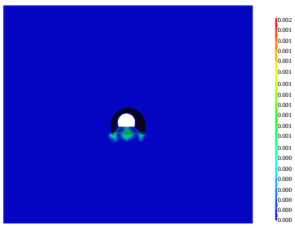

(c) Plastic deformation

Figure 9: Tunnel deformation during initial lining

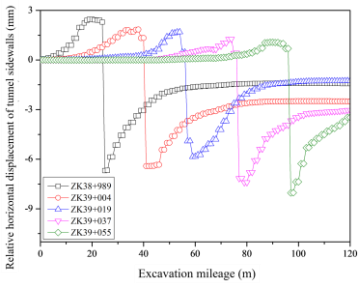

(a) Relative displacement of tunnel sidewalls

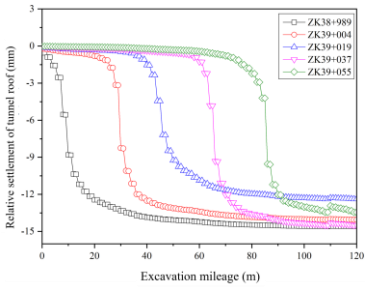

(b) Displacement of tunnel roof

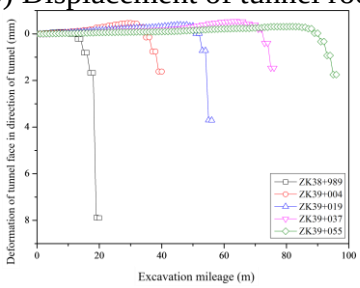

(c) Deformation of tunnel face

Figure 10: Dynamic change in tunnel deformation with excavation

(a) Tensile stress (b) Compressive stress

Figure 11: Initial lining internal forces

From the results of deformation and internal forces obtained from the finite element simulation analysis, it can be seen that under the initial lining structure, the plastic deformation of the surrounding rock is small, and the plastic damage zone is small. The internal forces of the lining are mainly compressive stress, with a partial tension stress zone appearing at the top of the lining, but the tension stress is relatively small. The trend of tunnel roof displacement is consistent with the relative displacement of tunnel sidewalls and deformation of the tunnel face, but the differences between them are relatively small. This is because the vertical displacement of the tunnel roof is strongly restricted by the surrounding rock mass, and the differences in vertical displacement of the tunnel roof are reduced by the effect of the lining structure. Based on the stress and deformation analysis results, the stability of the rock mass in the Dongpo Tunnel can be preliminarily determined to be good.

5. Conclusion

Based on digital twin technology, this study acquires information on the tunnel face using the drilling and blasting method and establishes a rock mass classification and information inference model based on Bayesian theory. The method is successfully applied to the Dongpo Tunnel, and the stability of the tunnel is analysed based on the inferred geological information. The main conclusions are as follows:

(1) The application of 3D laser scanning and point cloud data reconstruction techniques in information acquisition of tunnel faces has good results. Based on the reconstructed model, geometric information of rock masses, such as structural plane spacing, roughness, pathline length, and joint inclination, can be obtained.

(2) By combining 260 sets of rock mass information with Bayesian networks and junction tree

algorithms, an intelligent rock mass classification model applicable to GSI, RMR, and BQ is constructed. Based on this model, the accuracy rate of BQ standard applications in Dongpo Tunnel is 100%, and the other two are above 85%.

(3) Based on prior rock mass information and on-site test results, a formula relating the rock mass deformation modulus and classification criteria can be established. By using Bayesian inference combined with MCMC simulation, the posterior probability distribution of the rock mass deformation modulus can be obtained, thereby achieving a method to infer the rock mass deformation modulus based on field measurements and empirical information.

References

[1] Yu Jia, Zhong Denghua, Ren Bingyu, et al. Probabilistic Risk Analysis of Diversion Tunnel Construction Simulation[J]. Computer-aided civil and infrastructure engineering, 2017, 32(9): 748-771.

[2] Van Eldert Jeroen, Funehag Johan, Saiang David, et al. Rock support prediction based on measurement while drilling technology[J]. Bulletin of engineering geology and the environment, 2021, 80(2): 1449-1465.

[3] Tao Fei, Xiao Bin, Qi Qinglin, et al. Digital twin modeling[J]. Journal of manufacturing systems, 2022, 64: 372-389.

[4] Zhu Hehua, Li Xiaojun. Digital underground space and engineering[J]. Chinese Journal of Rock Mechanics and Engineering, 2007, 26(11): 2277-2288.

[5] Chen Jianqin, Zhu Hehua, Li Xiaojun. Automatic extraction of discontinuity orientation from rock mass surface 3D point cloud[J]. Computers and Geosciences, 2016, 95: 18-31.

[6] Lee Jaewook, Lee Yonghwan, Hong Changhee. Development of Geospatial Data Acquisition, Modeling, and Service Technology for Digital Twin Implementation of Underground Utility Tunnel[J]. Applied sciences-Basel, 2023, 13(7): 4343.

[7] Yu Gang, Wang Yi, Mao Zeyu, et al. A digital twin-based decision analysis framework for operation and maintenance of tunnels[J]. Tunnelling and underground space technology, 2021, 116: 104125.

[8] Shen Yi, Jing Jiaxin, Li Xiaojun, et al. Holistic digital-twin-based framework to improve tunnel lighting environment: From methodology to application[J]. Building and environment, 2022, 224: 109562.

[9] Li Xiaojun, Tang Li, Ling Jiaxin, et al. Digital-twin-enabled JIT design of rock tunnel: Methodology and application[J]. Tunnelling and underground space technology, 2023, 140: 105307.

[10] Zhou Yahui. Structural homogeneity delineation of rock mass and risk analysis of rock mass quality[D]. Nanjing University of Science And Technology, 2015.

[11] Xiao Xin, Zhang Yangsong. Interval probability analysis of rock mass shear strength based on bayesian network[J]. Site investigation science and technology, 2016, 2: 5-10.

[12] Cai Ming. Rock mass characterization and rock property variability considerations for tunnel and cavern design[J]. Rock mechanics and rock engineering, 2011, 44(4): 379-399.

[13] Sari Mehmet. Incorporating variability and/or uncertainty of rock mass properties into GSI and RMi systems using Monte Carlo method[M]//Engineering Geology for Society and Territory-Volume 6. Springer, Cham, 2015: 843-849.

[14] Feng Xianda, Jimenez Rafael. Bayesian prediction of elastic modulus of intact rocks using their uniaxial compressive strength [J]. Engineering Geology, 2014, 173(5):32-40.

[15] Wang Yu, Aladejare Adeyemi Emman. Bayesian characterization of correlation between uniaxial compressive strength and Young's modulus of rock[J]. International Journal of Rock Mechanics & Mining Sciences, 2016, 85:10-19.

[16] Wang Yu, Aladejare Adeyemi Emman. Selection of site-specific regression model for characterization of uniaxial compressive strength of rock[J]. International Journal of Rock Mechanics & Mining Sciences, 2015, 75:73-81.

[17] Li Xiaojun, Chen Jianqin, Zhu Hehua. A new method for automated discontinuity trace mapping on rock mass 3D surface model[J]. Computers & Geosciences, 2016, 89: 118-131.

[18] Zhu Hehua, Wu Wei, Chen Jianqin, et al. Integration of three dimensional discontinuous deformation analysis (DDA) with binocular photogrammetry for stability analysis of tunnels in blocky rockmass[J]. Tunnelling and Underground Space Technology, 2016, 51:30-40.

[19] Zhu Hehua, Wu Wei, Li Xiaojun, et al. High-precision Acquisition, analysis and service of rock tunnel information based on iS3 platform[J]. Chinese Journal of Rock Mechanics and Engineering, 2017, 36(10):2350-2364.

[20] Hoek E, Brown E T. Practical estimates of rock mass strength[J]. International Journal of Rock Mechanics and Mining Sciences, 1997, 34(8): 1165-1186.

[21] Sonmez H., Ulusay R. Modifications to the geological strength index (GSI) and their applicability to stability of slopes [J]. International Journal of Rock Mechanics and Mining Sciences, 1999, 36(6): 743-760.

[22] Wu Aiqing, Liu Fuzheng. Advancement and application of the Standard of engineering classification of rock masses [J]. Chinese Journal of Rock Mechanics and Engineering, 2012, 31(8):1513-1523.

[23] Bieniawski T Z. Engineering classification of jointed rock masses [J]. Civil Engineer in South Africa, 1973, 15: 335-343.

[24] Celada B, Tardáguila I, Bieniawski Z T. Innovating Tunnel design by an improved experience-based RMR system [C]. Proceedings of the World Tunnel Congress 2014-Tunnels for a better Life, Foz do Iguaçu, Brazil, 2014.

[25] Zhang Qi, Huang Xianbin, Zhu Hehua, et al. Quantitative assessments of the correlations between rock mass rating (RMR) and geological strength index (GSI)[J]. Tunnelling and underground space technology, 2019, 83: 73-81.
[26] Feng Xianda, Jimenez Rafael. Estimation of deformation modulus of rock masses based on Bayesian model selection and Bayesian updating approach[J]. Engineering Geology, 2015, 199:19-27.
[27] Feng Xianda, Jimenez Rafael. Predicting tunnel squeezing with incomplete data using Bayesian networks[J]. Engineering Geology, 2015, 195:214-224.
[28] Acquah H D G. Comparison of Akaike information criterion (AIC) and Bayesian information criterion (BIC) in selection of an asymmetric price relationship[J]. Journal of Development and Agricultural Economics, 2010, 2(1): 001-006.
[29] Ang A, Tang W H. Probability concepts in engineering: Emphasis on applications to civil & environmental engineering [M]. Hoboken, NJ: Wiley, 2007.
[30] Metropolis N, Rosenbluth A W, Rosenbluth M N, et al. Equation of State Calculations by Fast Computing Machines[J]. Journal of Chemical Physics, 1953, 21(6):1087-1092.
[31] Hastings W K. Monte Carlo sampling methods using Markov chains and their applications[J]. Biometrika, 1970, 57(1): 97-109.
[32] Zhang Qi, Zhu Hehua, Huang Xianbin, et al. A new rock mass rating method based on Mamdani fuzzy inference for rock tunnels [J]. Chinese Journal of Geotechnical Engineering, 2017, 39(11): 2116-2124.
[33] Gercek H. Poisson's ratio values for rocks [J]. International Journal of Rock Mechanics & Mining Sciences, 2007, 44(1):1-13.
[34] AASHTO. Standard Specifications for Highway Bridges. 14th edition, America Association of State Highway and Transportation Officials, Washington DC, 1989.
[35] Zhu Hehua, Huang Boqi, Zhang Qi, et al. Elastoplastic rock constitutive model based on generalized Hoek-Brown strength criterion and its numerical implementation[J]. Engineering mechanics, 2016(2):41-49.
[36] Zhu Hehua, Zhang Qi, Huang Boqi, et al. A constitutive model based on the modified generalized three-dimensional Hoek–Brown strength criterion[J]. International Journal of Rock Mechanics & Mining Sciences, 2017, 98:78-87.